Atmospheric Pollution Research 6 (2015) 682-695

Atmospheric Pollution Research

www.atmospolres.com

AERONET data–based determination of aerosol types

Fuyi Tan [1], Hwee San Lim [1], Khiruddin Abdullah [1], Tiem Leong Yoon [1], Brent Holben [2]

[1] *School of Physics, Universiti Sains Malaysia, Malaysia*
[2] *NASA Goddard Space Flight Center, USA*

ABSTRACT

Aerosols are among the most interesting topics investigated by researchers because of their complicated characteristics and poor quantification. Moreover, significant uncertainties are associated with changes in the Earth's radiation budget. Previous studies have shown numerous difficulties and challenges in quantifying aerosol influences. In addition, the heterogeneity from aerosol loading and properties, including spatial, temporal, size, and composition features, presents a challenge. In this study, we investigated aerosol characteristics over two regions with different environmental conditions and aerosol sources. The study sites are Penang and Kuching in Malaysia, where a ground–based AErosol RObotic NETwork (AERONET) sun–photometer was deployed. The types of aerosol, such as biomass burning, urban/industrial, marine, and dust aerosols, for both study sites were identified by analyzing aerosol optical depth and angstrom exponent. Seasonal monsoon variation results in different aerosol optical properties, characteristics, and types of aerosols that are dominant in Penang and Kuching. Seasonal monsoon flow trend patterns from a seven–day back–trajectory frequency plotted by the Hybrid Single–Particle Lagrangian Integrated Trajectory model illustrated the distinct origins of trans–boundary aerosol sources. Finally, we improved our findings in Malaysian sites using the AERONET data from Singapore and Indonesia. Similarities in the optical properties of aerosols and the distribution types (referred to as homogeneous aerosol) were observed in the Penang–Singapore and the Kuching–Pontianak sites. The dominant aerosol distribution types were completely different for locations in the western (Penang–Singapore) and eastern (Kuching–Pontianak) parts of the South China Sea. This is a result of spatial and temporal heterogeneity. The spatial and temporal heterogeneities for the western and eastern portions of South China Sea provide information on the natural or anthropogenic processes that take place.

Keywords: *Seasonal monsoon, aerosol, aerosol optical depth (AOD), angstrom exponent, precipitable water (PW)*

doi: 10.5094/APR.2015.077

Corresponding Author:
Fuyi Tan
☎ : *+60-194721521*
🖷 : *+60-46579150*
✉ : *fuyitan@yahoo.com*
tf09_phy061@student.usm.my

Article History:
Received: 21 June 2014
Revised: 28 January 2015
Accepted: 29 January 2015

1. Introduction

Understanding atmospheric aerosols is crucial for climate change dynamics. Owing to the presence of large uncertainty on aerosol reports by the Intergovernmental Panel for Climate Change (IPCC) 2007 on radiative forcing of climate between 1750 and 2005, the influence of the anthropogenic and natural forcing agents of aerosol on climate dynamics remains unclear and is an active area of scientific research (IPCC, 2007). Even the most recent report by IPCC working group I in the fifth assessment report (IPCC, 2013) also cited the same problems, that is, aerosol interaction with radiation and the existence of clouds, which result in significant uncertainty because of the complex mixing of aerosols and their variation in large volumes of the atmosphere.

Aerosols remain poorly characterized because of the spatial and temporal variations of aerosols and of the existence of different aerosol types, which have different properties. As a result, the global impact of aerosols on the Earth's climate is difficult to quantify because of the lack of extensive and reliable measurements in most regions of the world (Hansen et al., 1997; Tripathi et al., 2005; Kaskaoutis et al., 2007; Kaskaoutis and Kambezidis, 2008; Russell et al., 2010). Many scientists believe that the origins of aerosol sources and their distribution in the atmosphere should be determined to understand why different locations have different aerosol types and are affected by environmental development, monsoon and southern oscillation variation, and seasonal change. The trans–boundary long–range transport of aerosols may interact with local aerosols, especially with cloud droplets, thus further enhancing the modification of their microphysical properties, such that precipitation processes and their radiative properties are influenced (Ichoku et al., 2004; Rosenfeld, 2007; Andreae and Rosenfeld, 2008; Lin et al., 2013).

With the large uncertainty in characterizing aerosols, a local study for every region is essential for verifying satellite imagery because the extraction of aerosol optical properties from remote sensing data has limited accuracy despite its capability to provide global–scale coverage of aerosol properties (Kaufman et al., 2002; Levy et al., 2005; Tripathi et al., 2005; Gupta et al., 2013). Local studies on aerosol optical properties can be conducted by using reliable equipment, such as sun–photometers or sky radiometers (Holben et al., 1998; Remer et al., 2008; Salinas et al., 2009). However, these methods are limited to space coverage, unlike satellite imagery. Therefore, ground– and space–based measurements are complementary in performing reliable and comprehensive studies on atmospheric aerosols.

Characterization of aerosol properties is important because of the rapid growth of both population and economic activities, which cause the anthropogenic aerosol emission rates to increase as a result of the increases in fossil–fuel combustion and biomass burning. These pollutants directly affect the climate and, at the same time, increasing the haze, fog, and cloudy conditions (Mukai et al., 2006), which decrease visibility, particularly under high turbidity. According to Salinas et al. (2009), Asian sources are known to differ from those in Europe or North America. More absorbing soot and organic components are added to the Asia Pacific atmosphere because of substantially greater coal and biomass burning emissions and long–range transport by wind

(Lelieveld et al., 2001; Huebert et al., 2003; Seinfeld et al., 2004). In Singapore, industrial and fossil fuel combustion from energy stations and mobile vehicles are the major anthropogenic aerosols, as well as the biomass burning aerosol from neighboring countries at a certain period of the year (Salinas et al., 2009).

According to an environmental quality report for Malaysia in 2010, power plants (main pollutants emitted are nitrogen dioxide and sulfur dioxide), motor vehicles (main pollutant emitted is carbon monoxide), and industries (main pollutant emitted is particulate matter) are the major air pollutants in Malaysia (DOE, 2010). The major pollutants of concern in Malaysia are ground–level ozone and particulate matter that is less than 10 μm (PM_{10}), with PM_{10} being dominant most of the time. Moreover, PM_{10} value will increase abruptly during trans–boundary haze pollution from Central Sumatra, Indonesia, especially during the southwest monsoon period (June to September).

In this study, we intend to determine the sources and origin of the aerosol types distributed in the Penang and Kuching regions, which have different environmental conditions. In additional, the aerosols for both regions are investigated with respect to seasonal change, and the major dominant aerosol type is determined according to ground–based sun–photometer measurement from the AErosol RObotic NETwork (AERONET) database.

2. Methodology

The study sites are located in Penang, Peninsular Malaysia and Kuching, East Malaysia; a ground–based AERONET sun photometer was available for each site [Figure S1, see the Supporting Material (SM)]. The northern and southern parts of Southeast Asia respectively span from 8 °N to 28 °N and 10 °S to 8 °N for longitudes between 90 and 130 °E. Level 2 AERONET data were used in this study because they were cloud–screened and verified. Sun–photometer made direct sun measurements every 15 min at 340, 380, 440, 500, 675, 870, 940 and 1 020 nm (includes the 1 640 nm channel in Cimel version 5). These solar extinction measurements are used to compute aerosol optical depth (AOD). Typically the estimated uncertainty in computed AOD from a newly calibrated field instrument under cloud–free conditions is approximately ±0.010 to ±0.021, which is spectrally dependent with higher errors in the UV (<440 nm) (Holben et al., 1998; Eck et al., 1999). Angstrom exponent can be retrieved from AODs. Rather than calculating angstrom exponent on two wavelengths, as is traditionally done, 4 or more were used to plot for the AOD vs. wavelength in log space and making a linear fit of the data to retrieve the angstrom exponent. Thus if one channel is miscalibrated by 0.02 but the others are spot on, the angstrom exponent is less affected by the one bad channel. Normally very low AOD values may cause significant errors in AE. To minimize these errors, only AOD values larger than 0.05 at 500 nm were adopted. In our dataset, approximately 95% data recorded are AOD values larger than 0.1 at 500 nm. The remaining are AOD values in between 0.05 and 0.10.

In this study, we divided our dataset into four groups based on the seasonal monsoon (Awang et al., 2000; Babu et al., 2007; Moorthy et al., 2007; Kumar and Devara, 2012; Xian et al., 2013) as follows: (i) December to March (northeast monsoon), (ii) April to May (pre–monsoon), (iii) June to September (southwest monsoon), and (iv) October to November (post–monsoon). Meanwhile, the "overall" data were also analyzed for the entire study period. In this study, data obtained for Penang (Kuching) site is for the year 2012 (2011). The post–monsoon (pre–monsoon) period is not discussed for Penang (Kuching) because no data are available for that period. The aerosol optical properties of aerosols for the study sites on each monsoon season were identified by analyzing the AOD_500 and $angstrom_{440–870}$ based on their frequency distribution patterns. The frequency distribution patterns of PW (in cm) shows the amount of water content in the atmospheric column. Additionally, the aerosol distribution patterns over Penang in each monsoonal period were quantitatively identified according to the scattering plots of the angstrom exponent against aerosol optical depth (AOD). Therefore, the variations in aerosol characteristics could be inter–annually investigated to determine the aerosol types for different periods or those that were sustained throughout the year. However, the sites in Penang and Kuching lack a complete dataset of Level 2 AERONET data; hence, only four groups were considered for these sites. We could generally and subjectively compare the data. The seven–day back–trajectory frequency seasonal plot by the Hybrid Single–Particle Lagrangian Integrated Trajectory (HYSPLIT_4) model (Draxler and Hess, 1998) was used to describe the aerosol sources because of its suitability to simulate air–mass movement. The results obtained for Penang were compared against that of Singapore, while that of Kuching against Pontianak. Singapore and Pontianak were chosen due to (i) they have a complete annual Level 2 AERONET data, (ii) their proximity to the sites of comparison, (iii) similar environmental factors between the sites being compared.

3. Results and Discussion

3.1. Climatology of Penang and Kuching

The climatology data for Penang and Kuching is obtained from the website, e.g. (GSFC, 2014) for year 2012 and 2011 respectively. As shown in Figure S2 (see the SM) the AOD value at shorter wavelengths between 500 nm and 340 nm (visible in the ultraviolet wavelength portion) is obviously higher than that at longer wavelengths from 670 nm to 1 020 nm (visible in the near–infrared wavelength portion). This condition can be attributed to the fact that fine mode particles dominate the atmosphere because small particles are more efficiently scattered at shorter wavelengths than at longer wavelengths (Kaskaoutis et al., 2007). In Figure S2a (see the SM), the AOD value in Penang increases significantly during the southwest monsoon period, two peaks were found in June and August. Another peak is found in March during the northeast monsoon. During the inter–annual southwest monsoon period, smoke (biomass burning aerosol) is transported from Sumatra, Indonesia, to the study sites. Therefore, the fine biomass burning aerosols have a greater effect on the AOD in the ultraviolet than in the near–infrared wavelengths (Schuster et al., 2006). This phenomenon is obviously observed at AOD_340, which increases by a factor of ~2.7 from April to June in comparison with an increase by ~1.9 for AOD_1020. Meanwhile, Penang seldom has a very good air quality because the AOD_440 value is almost always higher than 0.1 in the study site records. Under clean background conditions, AOD value should be less than 0.05 at AOD_440 nm (Toledano et al., 2007) or pure atmospheric conditions should be between 0.04 and 0.06 (Smirnov et al., 1995). Kuching is also affected by the open burning activities from Kalimantan, Indonesia, during the inter–annual southwest monsoon period (refer to Figure S2b in the SM). The AOD value achieved the peak in August. Meanwhile, this site is also dominated by fine mode aerosol (smoke) because the AOD value at wavelengths shorter than 500 nm are significantly higher than that at longer than 500 nm, and AOD_340 increases by a factor of ~3.8 from April to August in comparison with ~3.5 for AOD_1020.

3.2. Temporal evolution for AOD, angstrom exponent, and PW

Penang. Figure 1a shows the spectral variation of AOD values at certain times in Penang. High, medium, and low fluctuations are observed during the southwest, northeast, and pre–monsoon periods. The high fluctuation of AOD during the southwest monsoon period (between June and September) is attributed to the intermittent open burning activities committed locally and from neighboring country, i.e., Indonesia. The Malaysia Meteorological Department (MMD) reported that rainfall amount in this period is the lowest of the year (MOSTI, 2012). Independently, recorded PW (the water content in the

atmospheric column), as depicted in Figure 1c, shows that in this period the PW occurs more frequently at values of less than 5.0 cm.

Meanwhile, the angstrom$_{440–870}$ in Figure 1b shows that the majority of the data was recorded between 1.3 and 1.7, indicating that the fine mode particles are dominant within this period. During the northeast monsoon, the average AOD recorded is lower than that during the southwest monsoon but higher than that during the pre–monsoon periods. This is because during this monsoon transition period, the winds are light and variable. Therefore, thunderstorms that develop in the afternoon wash out the aerosols in the atmosphere, thus explaining why the pre–monsoon period shows that the majority of records of AOD_500 are lower than 0.3 and that PW was approximately 5.0 cm for this time of the year, as proposed by Eck et al. (2010).

Kuching. During the southwest monsoon period, two peaks of AOD_500 were found at some days of August and September (Figure 2a). The second peak in September has a longer period than the first one but is much lower on the AOD_500 value. In addition, both of these peaks during the southwest monsoon were recorded when the PW is recorded as a lower value than any other time (compare Figures 2a and 2c). The leftover time for both post–monsoon and northeast monsoon also shows small variation of AOD_500. However, angstrom$_{440–870}$ was highly varied in all the seasonal monsoons (Figure 2b), with a seasonal standard deviation of ~0.21–0.27, showing no obvious sign of correlation when compared with the corresponding AOD and PW data. During the two peaks of AOD_500 (Figure 2a), the angstrom value was mainly higher than 1.2, implying that fine mode aerosols can be attributed to the transported smoke from the open burning activities because hotspot counts correspond to high AOD value (Jalal et al., 2012). Moreover, the lowest AOD_500 was observed during the post–monsoon period. During this post–monsoon period, the PW was high but AOD_500 was low, thus explaining why the raining event had washed out the aerosol in the sky.

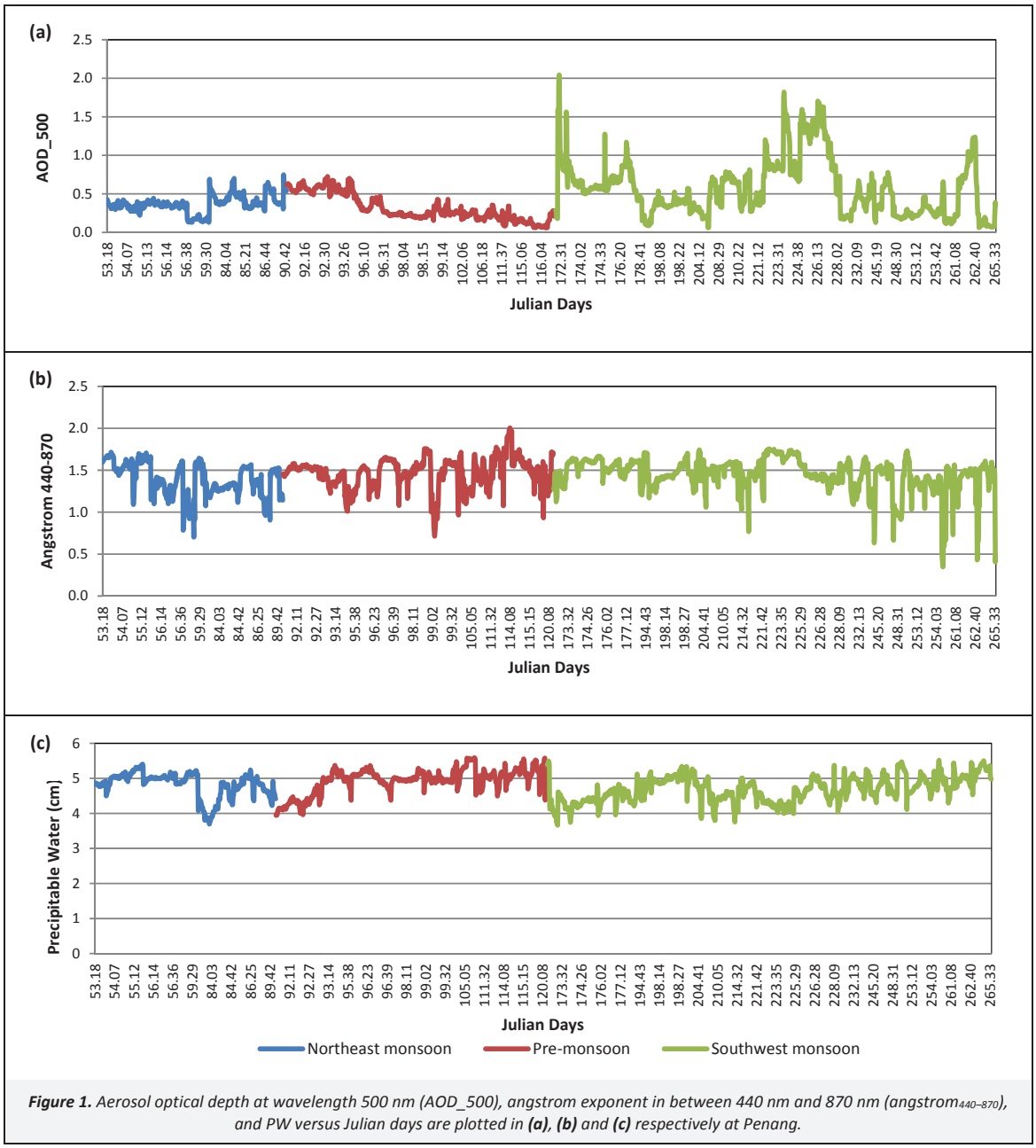

Figure 1. *Aerosol optical depth at wavelength 500 nm (AOD_500), angstrom exponent in between 440 nm and 870 nm (angstrom$_{440–870}$), and PW versus Julian days are plotted in* ***(a)****,* ***(b)*** *and* ***(c)*** *respectively at Penang.*

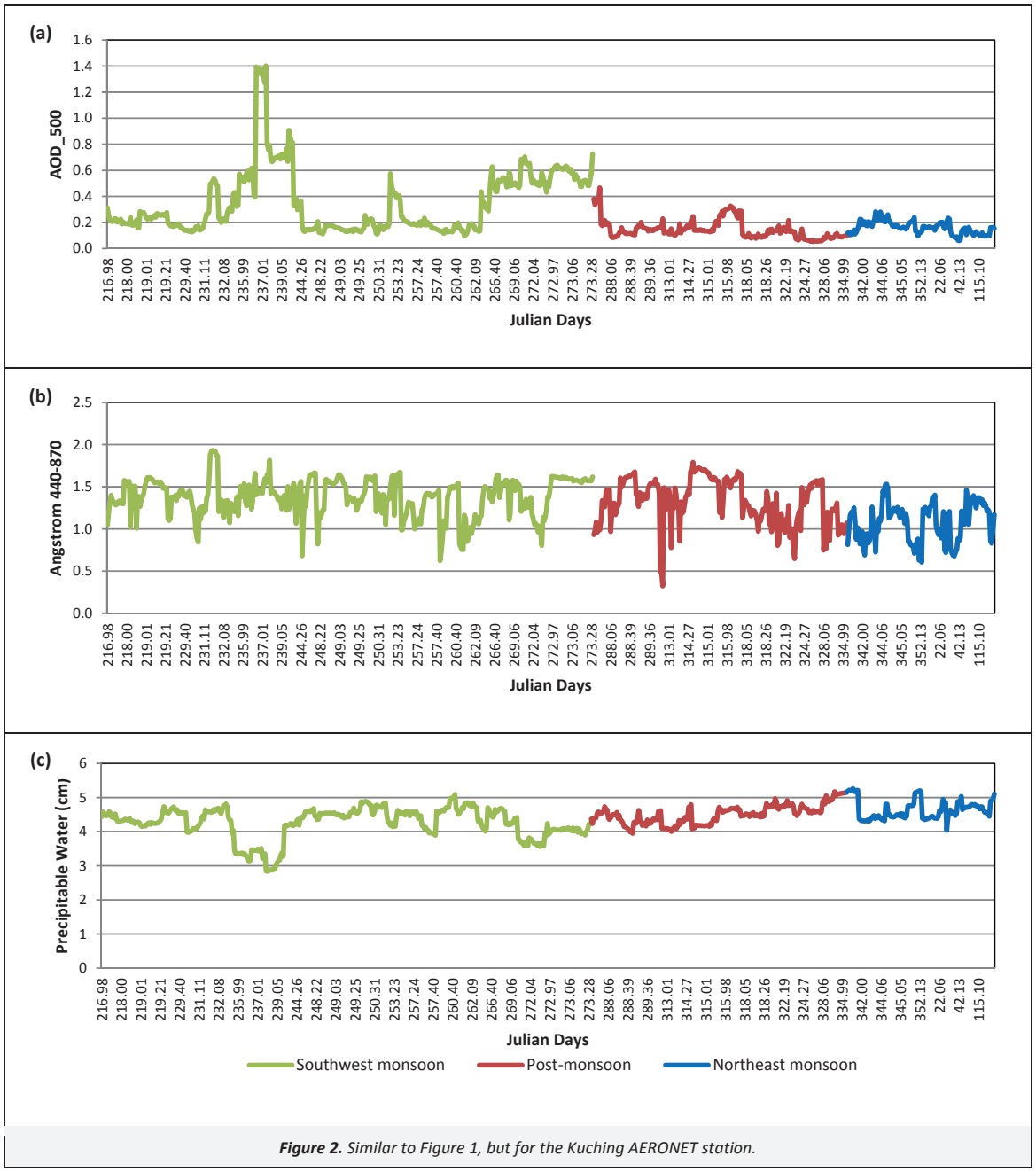

Figure 2. *Similar to Figure 1, but for the Kuching AERONET station.*

3.3. Seasonal variation of AOD, angstrom exponent, and PW based frequency distribution patterns

To determine aerosol properties further, the relative frequency distributions of the aerosols in the atmospheres of Penang and Kuching are plotted in Figures 3 and 4, respectively. Relative frequency is calculated on the basis of the accumulation of AOD_500, angstrom$_{440–870}$, and PW during seasonal monsoon change. These frequency histograms can reveal how optical properties change with the seasons and help to identify aerosol types (Smirnov et al., 2002a; Pace et al., 2006; Salinas et al., 2009; Smirnov et al., 2011).

Penang. In Figures 3a to 3f, the overall aerosol properties results for Penang show the mainly distributed AOD value is between 0.2 and 0.6 (>77% of frequency occurrence), and the angstrom value is between 1.3 and 1.9 (>85% of frequency occurrence) with PW value between 4.5 and 5.5 cm (>96% of frequency occurrence). According to Okulov et al. (2002), the criteria for atmosphere to be in humid or moist condition is when PW>4.0 cm. Otherwise the atmosphere is in dry condition. The climate in Penang is always humid. This is consistent with the observation in Figures 3c and 3f, in which out of the all PW measured in a year, 96% has a value of more than 4.0 cm). The results of occurrence frequency of PW less than 4.0 cm in 2012 was recorded twice as higher in the northeast monsoon (~12%) than southwest monsoon (~6%) (Figure 3c).

The high value of angstrom$_{440–870}$ shows that this study site is minimally affected by coarse particles, such as dust (Figures 3b and 3e). The peak of AOD is approximately 0.3 (0.4), but the value varies between 0.1 and 0.9 (0.2 and 0.8) for pre– (northeast) monsoon (refer to Figures 3a and 3d). However, during the southwest monsoon, the peak of AOD is 0.3 with a wider range from 0.1 to 1.8 (Figure 3a). The multiple peaks in Figure 3d indicate the presence of various aerosol populations because AOD

histograms are normally expected to follow a log–normal distribution pattern (Salinas et al., 2009).

A parallel set of graphs of the angstrom exponent displays an unobvious seasonal trend because more than 99% out of the total occurrence of angstrom$_{440–870}$ is within 1 to 2, which clearly explains why the study site is less affected by coarse aerosols (Figure 3b). This condition can be attributed to the fact that the environment of the study site does not have a desert area and is far from desert areas, which hinder the transport of dust to the study site. However, a slightly different angstrom moving trend was observed during the northeast monsoon period because two noticeable peaks were found and distinguished from those in the other period (refer to the blue curve in Figure 3e). We strongly believe that the aerosol origins from the northern region of Southeast Asia, especially from Indochina, and are transported by the monsoon wind. Aerosol in the northern region has been extensively studied under program of Seven South–East Asia Studies (7–SEAS) (Lin et al., 2013). Northern SEA suffers active biomass burning activities during the northeast monsoon period, usually reaching peak intensity in March. From the conceptual model, they found that biomass burning aerosols originating from Indochina are uplifted and transported in high– and low–level pathways by westerly and northeast monsoon flows, which lead the aerosols toward the southwest direction. We thus expect that these aerosols will continue to move toward our study site as wind circulation tends to blow toward the southwest direction [refer to the monthly mean streamline charts 1979–2010 of Lin et al. (2013)]. These transported aerosols were finally mixed with the local aerosols.

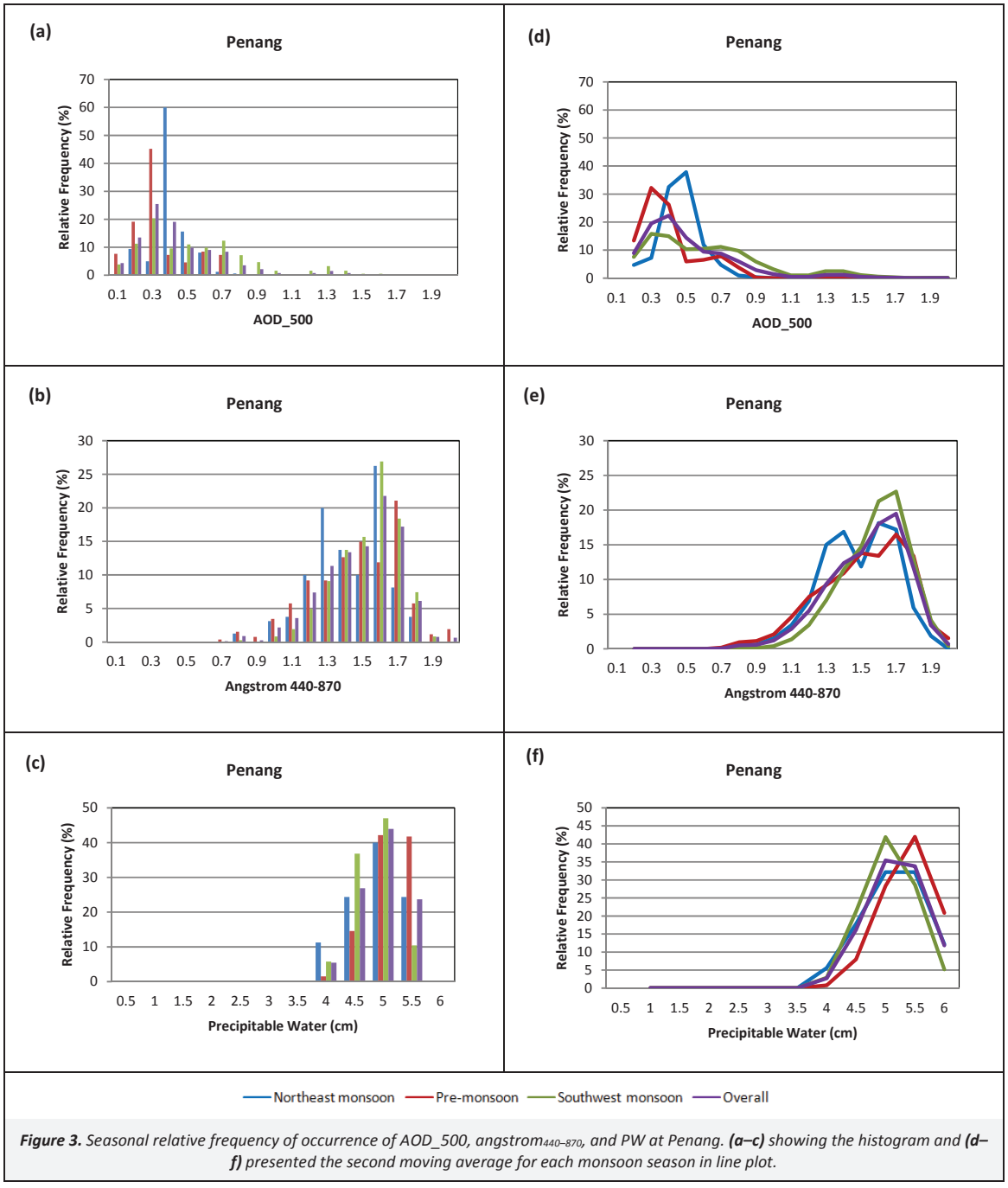

Figure 3. *Seasonal relative frequency of occurrence of AOD_500, angstrom$_{440–870}$, and PW at Penang.* ***(a–c)*** *showing the histogram and* ***(d–f)*** *presented the second moving average for each monsoon season in line plot.*

During the southwest monsoon, the angstrom value in the Penang tends to distribute between 1.3 and 1.6, which represents biomass burning aerosols (Holben et al., 2001; Gerasopoulos et al., 2003; Toledano et al., 2007), the origin of which are local sources and the neighboring country, Indonesia.

Kuching. The maximum peaks of AOD for overall period are primarily at value 0.2 (approximately 47% out of total occurrence), which indicates that the Kuching site is less polluted than the Penang site, except during the southwest monsoon period because of the open burning activities, due to which maximum AOD value can reach approximately 1.6 (Figure 4a). Moreover, the cleanest sky was also found during the post–monsoon season, when the majority of records are distributed between 0.1 and 0.2. This result is the same as that obtained from the Penang site because the aerosols were washed out during this season (as discussed in Figure 1). The AOD_500 frequency histogram at Kuching site was similar to that in the Penang site because during the southwest monsoon period, two peaks are found at approximately 0.3 and between 0.6 and 0.7 (Figures 3a and 4a). During the post–monsoon period, AOD at Kuching tends to clutter at smaller values. The PW distribution showed that the atmosphere at Kuching was the driest during the southwest monsoon and the wettest during the northeast monsoon period (Figures 4c and 4f).

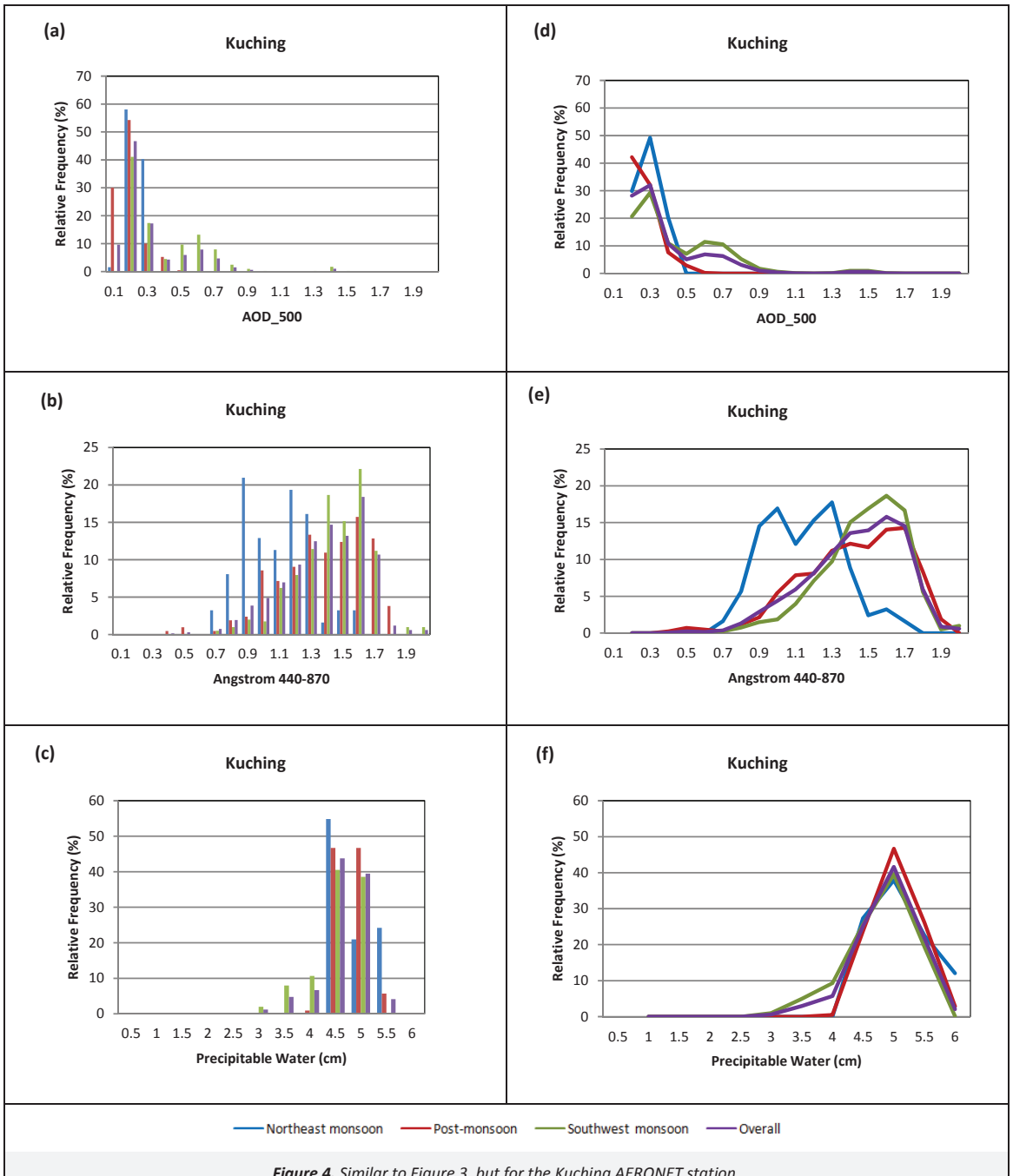

Figure 4. *Similar to Figure 3, but for the Kuching AERONET station.*

Comparison between Penang and Kuching results. Both sites of the Penang and Kuching, we observe that the relative frequency of AOD during the southwest and northeast monsoon always shifts to a higher AOD than that during the inter–monsoon season. Although the dataset obtained was for a different year for both study areas, the relative frequency distribution of angstrom at Penang and Kuching shows similar distribution patterns for monsoons and inter–monsoon periods (in Figures 3b, 3e and 4b, 4e). For example, (i) during the inter–monsoon period, the relative frequency of angstrom exponent value was widely distributed compared with that during other periods for both study sites (the broad or wide range of angstrom exponent value during the inter–monsoon indicated that the aerosols are characterized under complex conditions (Smirnov et al., 2002a)), (ii) angstrom exponent in both Penang and Kuching during the southwest monsoon is distributed from 1.0 to 1.6, (peak of relative frequency occurs at 1.6 angstrom), and the value of peak relative frequency is higher than the corresponding peak frequencies from the other seasonal monsoons, (iii) two noticeable peaks and similar distribution pattern is found during the northeast monsoon period but the only difference is that the angstrom peak values at Kuching (0.9 to 1.2) are significantly lower than that in Penang (1.3 to 1.6). This information significantly indicated that aerosol properties varied with the season.

3.4. Seasonal discrimination of aerosol types based on relationship between AOD and angstrom exponent

Based on the literature review, we observed that aerosol classification by using AOD (τ) and angstrom exponent (α) has been widely studied. The α–τ scatter plot is a very helpful tool to classify aerosol type. AOD gives information about the aerosol loading in the atmospheric column by extinction of radiation rate of certain wavelength, whereas the angstrom exponent provides aerosol size determination in coarse and fine modes from the slope of wavelength depending on the AOD in the logarithmic coordinates. Additionally, both τ and α should be used to characterize aerosol properties because both of them depend strongly on wavelength (Holben et al., 2001). Therefore, the α–τ scatter plot may indicate the amount and dimension of the observed aerosol and aerosol distribution pattern has been grouped into a few clusters from the interpretation to determine aerosol species. Normally, aerosol classes will be divided into (i) desert dust (DA), (ii) maritime (MA), (iii) continental/urban/industrial (UIA), (iv) biomass burning (BMA), and (v) mixed aerosols (difficult to clearly verify among each other, simply referred as MIXA) (Ichoku et al., 2004). Aerosol classification by using α–τ scatter plots was extensively analyzed, as shown in Text S1 (see the SM).

Based on threshold suggestion by Pace et al. (2006), Kaskaoutis et al. (2007) and Smirnov et al. (2002b, 2003) (see the SM, Text S2), the results shown in Figure S3 (see the SM) indicate that several suggested threshold values were inappropriate for Malaysia. The suggested threshold cannot discriminate aerosol types in both Penang and Kuching sites because (i) Penang is an island surrounded by sea water, and (ii) Kuching site is near the coastal area, such that MA should be high, not 0% as in the result in Figures S3a to S3c, with Figure S3d also reflecting a small amount. Although dust aerosol is recorded as 0% and BMA between 11–45% is reasonable but there were dominant by MIXA, which means that we are unable to distinguish this type. Therefore, the result is meaningless if we have large uncertainty in identifying major or dominant distribution aerosols in the study sites. Thus, other options suggested by other researchers should be considered such as by Toledano et al. (2007), Salinas et al. (2009) and Jalal et al. (2012) (see the SM, Text S3).

To achieve better identification of aerosol distribution types in our study sites, a comparison is necessary to choose a better threshold range to discriminate aerosol types based on α–τ scatter plots (refer to Figures S6 and S7 for Penang and Kuching, respectively, see the SM). Interestingly, we found that threshold range suggested by the Toledano et al. (2007) provided the least MIXA from Figures 5a and 5e compared to that provided by others. During the southwest monsoon period, Toledano et al. (2007) also provided the highest accumulative relative frequency for BMA in the red bar (Figures 5b and 5f), which indicates that haze occurs in this period, correspond to the results we discussed in Figures 1 and 3 for Penang and Figures 2 and 4 for Kuching site. In Figures 3b, 3e and 4b, 4e the relative frequency histogram shows the angstrom distribution patterns during the northeast monsoon periods for both sites with two noticeable peaks, but Kuching has a lower angstrom value at approximately 0.9 to 1.2 than Penang at approximately 1.3 to 1.6. These results can be explained by Figures 5c and 5g for Penang and Kuching, respectively. In Penang, the blue curve indicates that the aerosols are dominated by finer particles (Figure 3e), whereas Figure 5c also shows dominance by well–known fine mode particles of UIA (23%) and BMA (29%). However, a large amount of aerosol cannot be determined and is thus referred to as MIXA (39%). On the other hand, the coarser particles at Kuching site (blue curve in Figure 4e) are also well defined in Figure 5g as they are dominated by coarse particles such as MA (77%) and DA (3%) with fine particles of UIA (19%). The aforementioned results indicate that the different values of the angstrom at the observed peaks in Penang (finer particles) and Kuching (coarser particles) are possibly due to different dominant aerosols types. Nevertheless, we cannot definitely determine the more appropriate threshold ranges for our study sites during the inter–monsoon periods (Figures 5d and 5h) because all ranges can be possibly true owing to the wider distribution range in Figures 3e and 4e (red curve). Overall, we can conclude that the thresholds provided by Toledano et al. (2007) are the typical threshold ranges for both of our study sites to examined aerosol types.

From the threshold criteria of AOD and angstrom scatter plot provided by Toledano et al. (2007) for aerosol type classification, we understand that the dominant aerosol types during the southwest monsoon periods is BMA at approximately 50%, and followed by UIA at approximately 30% in Penang (Figure 5b) because of very active open burning activities in Sumatra, Indonesia. However, MIXA reached as high as 40% in Penang during the northeast monsoon period, followed by BMA and UIA at approximately 23% and 28%, respectively (Figure 5c) owing to the trans–boundary aerosols from Indochina and Taiwan based on our analysis of the study by Lin et al. (2013). However, during the inter–monsoon period, UIA was the major aerosol distributed in Penang region, reaching about 49% out of the total, followed by MA at 22%, BMA at 15%, dust at 8%, and those that are not well defined at 6%. Obviously, the aerosol distributed in Penang region was highly dependent on seasonal change. However, UIA is always the most highly emitted pollutant for every season and thus directly affects the air quality in Malaysia. Moreover, BMA is one of the major pollutants in Penang (mainly local burning activities), which significantly faces serious haze problem during the southwest monsoon season (trans–boundary aerosols from Indonesia). These results are in line with the records from of the Department of Environment (DOE, 2010).

MA (~44%) was the dominant aerosol in Kuching, and the second highest aerosol type was UIA (~27%), followed by BMA at approximately 15% (refer to Figure 5e). MIXA was not found in large amounts in this region, and dust particles are the least contributor to the air pollution in Kuching because there is no desert area near the study site. Dust particles can be defined as those caused by the dust at the ground surface induced by vehicle transportation and construction.

During the southwest monsoon, open burning activity is usually very active in southern SEA. Hence BMA is expected to be the major aerosol contributor in Kuching in this season. However,

referring to Figure 5f, BMA (~25%) was not the only major aerosol type in Kuching. Instead, the contribution to aerosol is also dominated by UIA (~31%) and MA (~28%). This result is possibly due to missing data for June and July, during which a large amount of trans–boundary aerosol came from Kalimantan, Indonesia.

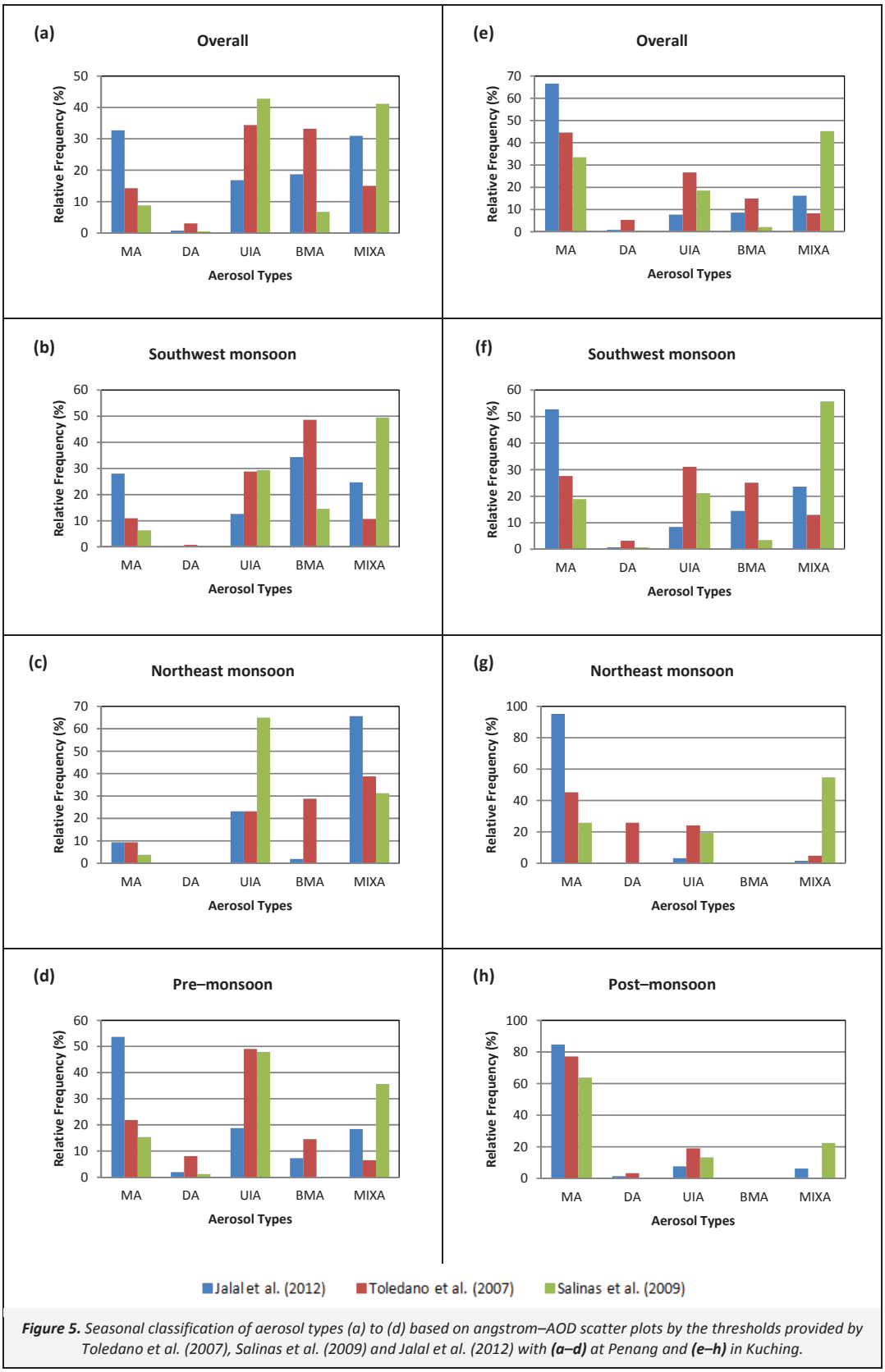

Figure 5. *Seasonal classification of aerosol types (a) to (d) based on angstrom–AOD scatter plots by the thresholds provided by Toledano et al. (2007), Salinas et al. (2009) and Jalal et al. (2012) with* ***(a–d)*** *at Penang and* ***(e–h)*** *in Kuching.*

During the northeast monsoon period, the dominant aerosol in Kuching was MA (~45%), followed by DA and UIA with approximately 25% and 24%, respectively (Figure 5g). Based on these dominant aerosols, we can clearly explain the features obtained from the blue curve in Figure 4e because their coarser MA and DA particles mixed with the finer UIA particles, such that the distribution pattern of two peaks is shown. We also strongly believe that the sources came from Indochina through the monsoon wind [as mentioned by Lin et al. (2013)], and the zero BMA recorded in this period is surprising. No BMA was found during this period because only the December 2011 dataset was considered, but according to Lin et al. (2013), the active biomass burning period should be between February and April annually. MA was the major aerosol type during the post–monsoon period. From our results, as high as 77% of aerosol is defined as MA in Kuching, followed by UIA at approximately 19% and 3% for dust particles, with other aerosol types accounting for less than 1% (Figure 5h).

The results show that UIA is one of the major pollutants in both Penang and Kuching sites throughout the monsoon periods. However, BMA (MA) is also often dominant in Penang (Kuching) throughout the year. Although MA is not the major aerosol type in Penang, it is consistently distributed over Penang region because the site is surrounded by sea water. Additionally, seasonal variation has caused different dominant aerosol types to be distributed in the sites. DA almost always is the least aerosol found in our study. Open burning around Kuching site was inactive from October to December 2011 because no BMA was found in our records (refer to Figures 5g and 5h), even from the thresholds provided by Toledano et al. (2007), Salinas et al. (2009) and Jalal et al. (2012). We understand that both sites have different dominant aerosol sources at different seasons.

3.5. Seasonal air parcel flow patterns from HYSPLIT_4 model is used to identify aerosols origin

From the 7 day back–trajectory frequency seasonal plot by HYSPLIT_4 model, the air parcel flow patterns are illustrated for each monsoon season in the value of percentage averaged in between ground surface to 5 000 m altitude (Figure 6). Figures 6a to 6c for Penang site during 2012 and Figures 6d to 6f for Kuching site during 2011 show similar air flow trend patterns. For example, Figures 6a and 6d show that the air flow trend is influenced by the southwest wind (called the southwest monsoon wind, occuring from June to September). Therefore, the aerosol source for Penang site comes from Andaman Sea in the Indian Ocean, Sumatra of Indonesia, Malacca Strait, and local areas, whereas Kuching site is affected by the aerosols generated from Java and Bali Sea, Kalimantan or Borneo, Indonesia, and local areas.

During the northeast monsoon period, the air parcel obviously flows southwestward from north of Southeast Asia, which significantly shows that the two different monsoon seasons provide totally diffferent aerosol sources to our study sites at Penang and Kuching in Figures 6b and 6e, respectively. Aerosols may form at the northern part of Southeast Asia, including Indochina, and is transported through South China Sea to reach Penang. Meanwhile, aerosol is also produced from the local region. The source origin of aerosols at Kuching was from local regions and transported from the northern region of Southeast Asia, especailly the Philippines, Taiwan, and east of China through South China Sea.

Figure 6c shows that the aerosol observed at Penang might come from the Malacca Strait, Andaman Sea in the Indian Ocean, northern and some eastern areas of Sumatra, western peninsular Malaysia, especially the local region marked in yellow. During the pre–monsoon period, the air flow patterns are similar to the southwest monsoon period, as shown in Figure 6a. However, the aerosol found at Kuching site during post–monsoon periods is near the regions of the southern part of South China Sea and litter from Java Sea, west of Kalimantan, and from local areas (refer to Figure 6f).

According to Figure 6, the significantly different seasonal patterns in relative frequency of occurrence of angstrom$_{440–870}$ in Penang and Kuching (in Figures 3b, 3e and 4b, 4e) for the northeast monsoon season are attributed to the mixing of the different sources from the northern part of Southeast Asia, including Indochina, Philippines, Taiwan, and Eastern China along with southern Southeast Asia (Malaysia and Indonesia) aerosols. Therefore, bimodal patterns are only obtained during the northeast monsoon period. However, aerosols originating at southern Southeast Asia during other monsoonal seasons are shown as a single peak pattern in Figures 3e and 4e. From this finding, the aerosols originating from northern Southeast Asia contains different sizes when emitted in the southern domain.

In addition, the aerosol emissions from the active open burning and/or forest fires in southern Southeast Asia is transported to our study sites by the southwest monsoon season (refer to Figures 6a and 6d), which supports the results obtained in Figures 5b and 5f. The findings indicate that BMA is dominant during this period. However, during the northeast monsoon, the local aerosol sources are mixed with multi–sources from Indochina (refer to Figure 6b). Thus, MIXA is primarily observed in Penang (refer to Figure 5c), whereas MA is a major aerosol type in Kuching because the long–range transport of the aerosols passes through the South China Sea, such that a large amount of MA is brought to the site (refer to Figures 6e and 5g). Therefore, we can observe that the aerosol types are not identical for the study sites. During the inter–monsoon season, the dominant aerosol types in Penang and Kuching are UIA and MA (refer to Figures 5d and 5h). During the inter–monsoon period, calm wind conditions resulted local sources, such as industrial emissions, to be trapped in the region, especially in Penang, which is the second largest city in Malaysia and one of the most industrially concentrated cities (larger yellow portion in Figures 6c and 6f than other monsoon period). Therefore, UIA is the major contributor to Penang during this season. However, MA is often the major aerosol type in Kuching because of its strategic location, but other aerosol types may vary according to seasonal changes.

3.6. Enhanced results in Malaysia via AERONET data from sites in Singapore and Pontianak, Indonesia Borneo

Comprehensive optical properties of aerosols and classifications have been analyzed for Penang and Kuching. However, the limited Level 2 AERONET data were insufficient to conclude the accuracy of these findings. As a means to check the consistency of these findings, we shall compare them against other locations that possess a more complete data, similar climate (tropic) and environment. These sites possess similar environments and a complete annual dataset for comparative purposes. The tropic climate normally has uniform temperature and pressure, high humidity and abundant rainfall. They should show similar seasonal monsoon changes. We therefore analyzed the data acquired from sites in Singapore (November 2006 to October 2013) and Pontianak, Indonesia (July 2012 to July 2013). In addition, Singapore and Pontianak have environmental features similar to those in Penang and Kuching, respectively. These sites possess similar environments and a complete annual dataset for comparative purposes.

Comparison of seasonal variation of AOD, angstrom exponent, and PW between Penang, Singapore, Kuching, and Pontianak. Figures 3a and Figures S4a (see the SM) show that the majority of AOD was between 0.2 and 0.4; the maximum was observed at 0.3. However, Singapore had a wide range of the relative frequency of AOD in during the post–monsoon, which was followed by the

frequency range during the southwest monsoon. Clear days were frequent in Kuching and Pontianak because majority of the AOD values ranged from 0.1 to 0.2 (Figure 4a and Figure S5a, see the SM). The AOD ranges in Kuching and Pontianak were wide during the southwest monsoon.

The results for Singapore and Pontianak revealed similar occurrences of the relative frequency of angstrom$_{440–870}$ for northeast monsoon period with those in Penang and Kuching, respectively [Figures S4e and S5e (see the SM) and Figures 3e and 4e]. Four of these study sites have wider ranges and high occurrences on small angstrom$_{440–870}$; coarse particles dominated during the northeast monsoon period. Penang, Singapore, and Kuching showed similar variation patterns, in which the maximum occurrence peak was located between 1.5 and 1.7. The most frequent occurrence peak of angstrom$_{440–870}$ was found in Penang, Singapore, and Kuching during the southwest monsoon. By contrast, the occurrence peak for pre–monsoon in Pontianak was shifted to 1.9.

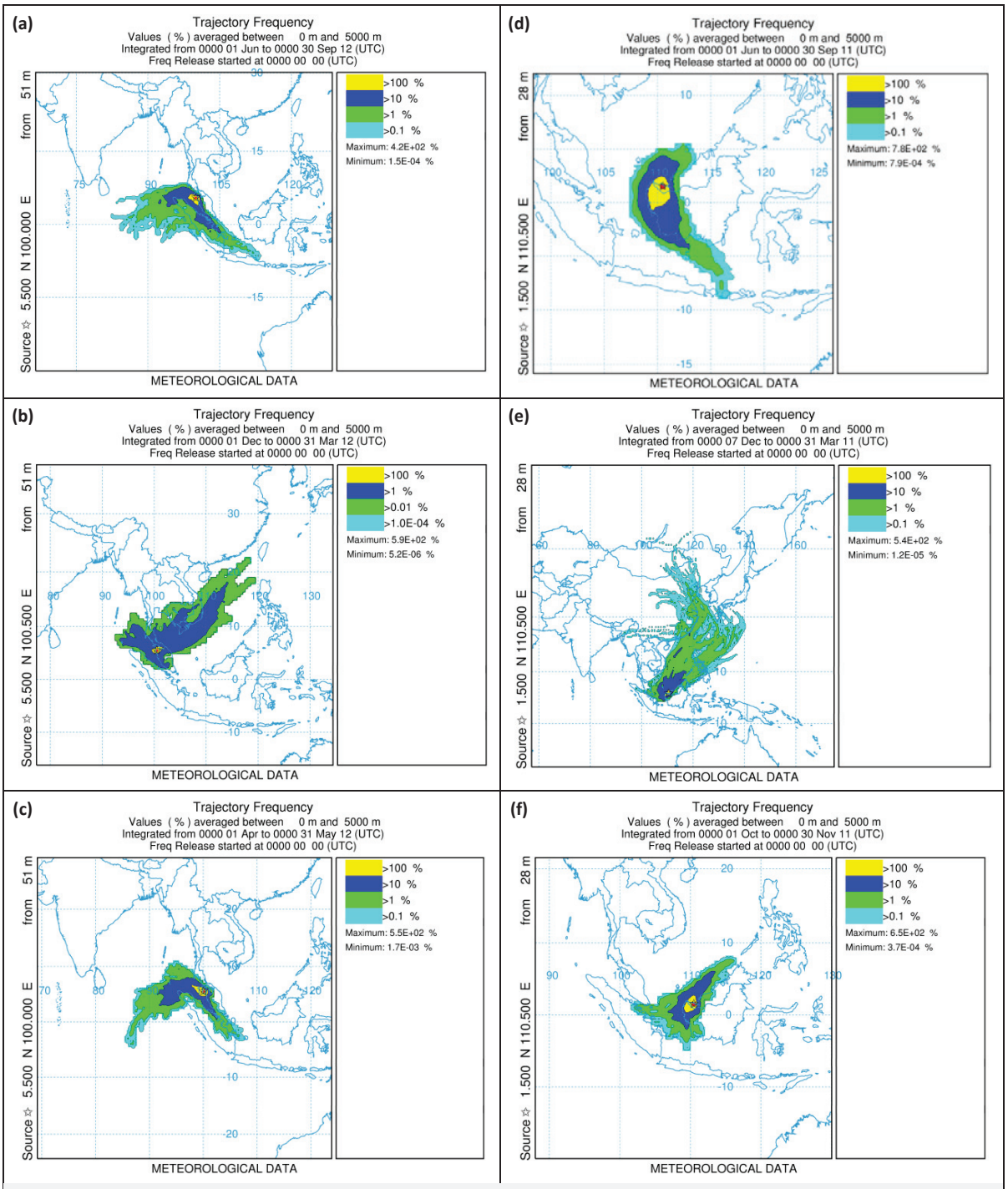

Figure 6. *Seven–day back–trajectory frequency seasonal plot by HYSPLIT_4 model during the southwest monsoon, northeast monsoon and inter–monsoon at Penang in 2012* ***(a–c)*** *and* ***(d–f)*** *at Kuching in 2011.*

Low PW occurred in Penang and Singapore during the northeast monsoon (see Figures 3c and 3f and Figures S4c and S4f in the SM). However, low PW in Kuching and Pontianak occurred during the southwest monsoon (see Figures 4c and 4f and Figures S5c and S5f in the SM). The water content in the atmosphere does not always exhibit a low value during the southwest monsoon in Southeast Asia. PW with higher values tend to occur more often in pre– and post–monsoon. Therefore, the water content in the atmospheric column is probably not exhibiting any direct relationship to the accumulation of precipitation amount. Therefore, the wettest and driest periods in Malaysia is indicated by the accumulation of precipitation amount but not the water content in the atmosphere. This finding is important for meteorological and aerosol–related studies.

Comparison of seasonal discrimination of aerosol types between Penang, Singapore, Kuching, and Pontianak. The results obtained in Section 3.4 revealed that the aerosol types in Penang and Kuching were efficiently identified using the α–τ scatter plots and threshold criteria by Toledano et al. (2007). Therefore, the same method for aerosol discrimination was applied to Singapore and Pontianak dataset. The scatter plots for Singapore and Pontianak are shown in Figure S8 (see the SM). Figure 7 shows the classifications for each seasonal monsoon for aerosol types were plotted for (a) Singapore, (b) Pontianak, (c) Penang, and (d) Kuching based on threshold of Toledano et al. (2007).

Figure 7 shows that the relative frequency distribution pattern of aerosol type is similar between Singapore and Penang; and Pontianak and Kuching. The dominant aerosol distributions were completely different for western (Penang and Singapore) and eastern (Kuching and Pontianak) portions of South China Sea (Figure S1). This phenomenon is known as spatial and temporal heterogeneity. The study sites located at the same latitude but in different longitude have different environmental and meteorological factors (Satheesh et al., 2006; Moorthy et al., 2013). The spatial and temporal heterogeneity for western and eastern parts of South China Sea are due to the differences in the natural or anthropogenic processes that occur locally and in neighboring areas. However, the relative frequencies for aerosol types were clearly distinguished between western and eastern parts of South China Sea.

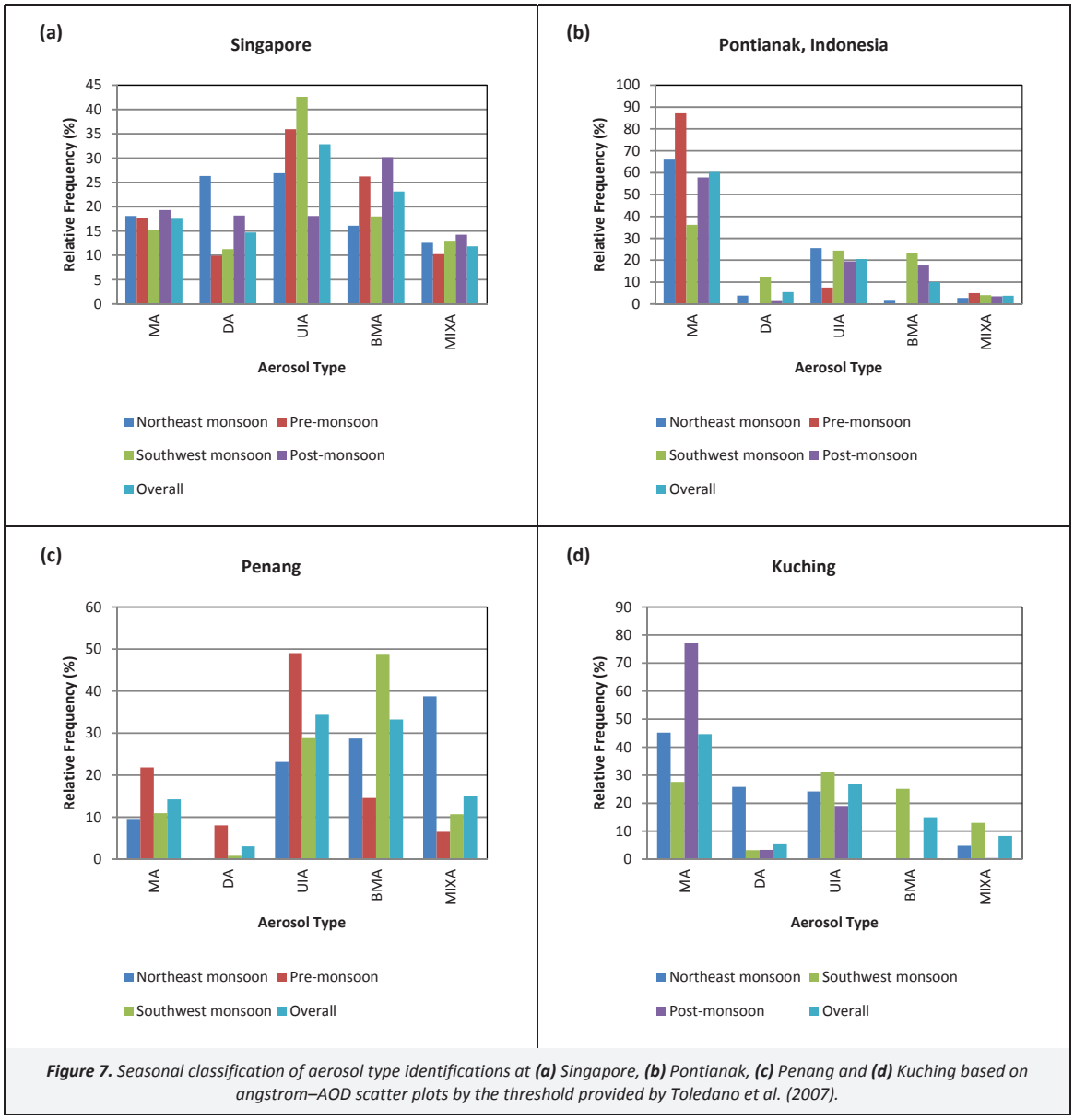

Figure 7. *Seasonal classification of aerosol type identifications at* ***(a)*** *Singapore,* ***(b)*** *Pontianak,* ***(c)*** *Penang and* ***(d)*** *Kuching based on angstrom–AOD scatter plots by the threshold provided by Toledano et al. (2007).*

Sumatra is located on the western site of Singapore and Penang Island. Both sites have similar meteorological factors such as monsoon circulation, therefore the trans–boundary aerosols such as BMA could be from the same origin. However, Figure 7a shows the two highest relative frequencies of BMA in Singapore occurred during the post–monsoon (30%) and pre–monsoon (26%). However, in Penang (Figure 7b), the two highest relative frequencies occurred in southwest monsoon (49%) and followed by northeast monsoon (28%). The difference in BMA dominant period between the two sites is possibly caused by time lag effect for the smoke aerosol to be transported to the sites from the sources in Sumatra. BMA is not occurring at a considerable level in Singapore during the northeast monsoon period because it is distant from northern SEA. Meanwhile the larger percentage of occurrence frequency of MIXA in Penang (~39%) as compared to Singapore during the northeast monsoon further indicates that the trans–boundary source was possibly from northern SEA. DA contributed to more than 10% of the air pollution in Singapore in each monsoon period. This parameter significant increased during the northeast monsoon period. However, DA is not an active aerosol contributor in Penang Island. DA has a higher occurrence frequency in Singapore in which the source was possibly from local construction sites (Chew et al., 2011). At Singapore UIA was one of the major pollutants throughout the years. This situation is similar to Penang because both sites are urban areas.

On the other hand, the aerosol distribution types in Pontianak and Kuching were similar because the most frequently occurred aerosol type was MA, followed by UIA (Figures 7b and 7d). The MA was significantly higher at Pontianak (88%) during the pre–monsoon, whereas at Kuching it was 78% during the post–monsoon. BMA was one of the major aerosol types in both Pontianak and Kuching during the southwest monsoon (between 23 and 25%). However it was not observed during the pre–monsoon period in both sites. MIXA was also not frequently observed in both sites.

In this study, the MA observed is not necessarily a major aerosol type for these sites. However, urbanization and high development rates have marked effects. The relative frequency of the BMA variation rate indicated that the air qualities in Penang and Singapore were frequently affected by open burning emissions in contrast to those in Pontianak and Kuching.

4. Conclusions

Seasonal variations in aerosol loading, type, and precipitable water have been studied for Penang and Kuching during the southwest and northeast monsoon and two inter–monsoons. Singapore and Potianak, of which a more complete data are available, are used as references in the comparison with the analysis results obtained for Penang and Kuching.

The dominant aerosol types were completely different for western (Penang and Singapore) and eastern (Kuching and Pontianak) portions of South China Sea due to spatial and temporal heterogeneity. This heterogeneity is due to the differences in natural or anthropogenic processes that occur locally and in neighboring areas. The dominant distribution types in each seasonal monsoon for Kuching and Pontianak were similar because the geographical locations of both sites are close to each other. However, the dominant aerosol types in the western side (Singapore and Penang) during different seasonal monsoon were not very similar. These differences may be due to the distant separation between them, and time lag effect of the trans–boundary aerosols.

BMA displays abrupt increases during the southwest monsoon period in southern Southeast Asia because of the active open burning activity in local areas and neighboring countries. During the northeast monsoon period, the aerosol optical properties, especially the size distribution pattern, were found to be unique compared to other monsoon seasons. During the northeast monsoon, the local aerosols might have mixed with the aerosols from the northern part of Southeast Asia transported by the northeast monsoon wind.

Dust particles contribute minimally to the emissions in Malaysia because the geographic location has no desert dust and is a great distance away from desert areas. However, the small amount of DA particles present in the data is believed to be caused by vehicles and construction activities.

MA observed is not necessarily a major aerosol type for these sites. However, urbanization and high development rates have marked effects. The relative frequency of the BMA variation rate indicated that the air qualities in Penang and Singapore were frequently affected by open burning emissions in contrast to those in Pontianak and Kuching.

A better understanding of the distribution and characteristics of major aerosol types helps to improve the accuracy of aerosol prediction model. However, AERONET stations in southern Southeast Asia are still a recent establishment, and the number of deployed sites are limited. Therefore, long–term observations and studies are necessary in order to identify aerosol distribution trends and their characteristics, especially for the Malaysian sites. Further studies should consider the hygroscopic and hydrophobic behavior of the distributed aerosols in Malaysia as the country is very humid and hot throughout the year. Such a climate may give rise to a different dynamics of aerosol interactions than that in other countries with different climatic and geographical behaviors.

Acknowledgments

The authors gratefully acknowledge the financial support provided by RU (Grant No. 1001/PFIZIK/811228) and RUI–PRGS grants (Grant No. 1001/PFIZIK/846083). The Universiti Sains Malaysia–Short Term Grant 304/PFIZIK/6310057 was likewise used to implement this project. The authors are also grateful to the members of the NASA Goddard Space Flight Center who helped with the set up and the site members who helped to maintain AERONET in Penang and Kuching. The authors also acknowledge Dr. Smimov from NASA for fruitful discussions on certain issues. The author also would like to thank Hui Qi Lim and Yeap Eng Choon who provided information for this study.

Supporting Material Available

Aerosol classification studies (Text S1), Threshold values from α–τ scatter plots for aerosol classification suggested by Smirnov et al. (2002b, 2003), Pace et al. (2006) and Kaskaoutis et al. (2007) (Text S2), Threshold values from α–τ scatter plots for aerosol classification suggested by Toledano et al. (2007), Salinas et al. (2009) and Jalal et al. (2012) (Text S3), Topography of Southeast Asia is illustrated in an elevation map from ASTER GDEM data with latitude of 1° S to 21° N and longitude of 94 °E to 128 °E. The four– and five–edged star, square and circle in the figure indicate the study sites of Penang, Singapore, Pontianak and Kuching, respectively (Figure S1), Climatology of AOD data at different wavelengths at a) Penang (2012) and b) Kuching (2011) (Figure S2), Classification of aerosol types based on thresholds provided by Pace et al. (2006) and Kaskaoutis et al. (2007) for a) and b) and Smirnov et al. (2002b, 2003) for c) and d) at Penang and Kuching, respectively (Figure S3), Seasonal relative frequency of occurrence of AOD_500, angstrom$_{440–870}$, and PW at Singapore. (a–c) showing the histogram and (d–f) presented the second moving average for each monsoon season in line plot (Figure S4), Similar to Figure S4, but for the Pontianak AERONET station (Figure S5). Scatter plot between AOD_440 and angstrom exponent at 440–870 nm for the

discrimination of different aerosol types over Penang. The aerosol types discrimination based on Jalal et al. (2012), Toledano et al. (2007), Salinas et al. (2009) are shown at (a–d), (e–h) and (i–l) respectively for the overall period, southwest monsoon, northeast monsoon and pre–monsoon (Figure S6). Scatter plot between AOD_440 and angstrom exponent at 440–870 nm for the discrimination of different aerosol types over Kuching. The aerosol types discrimination based on Jalal et al. (2012), Toledano et al. (2007), Salinas et al. (2009) are shown at (a–d), (e–h) and (i–l) respectively for the overall period, southwest monsoon, northeast monsoon and post–monsoon (Figure S7). Scatter plot between AOD_440 and angstrom exponent at 440–870 nm for the discrimination of different aerosol types over Singapore (a–e) and Pontianak (f–j). The aerosol types discrimination based on Toledano et al. (2007) for the overall period, southwest monsoon, pre–monsoon, northeast monsoon and post–monsoon (Figure S8). This information is available free of charge via the internet at http://www.atmospolres.com.

References

Andreae, M.O., Rosenfeld, D., 2008. Aerosol–cloud–precipitation interactions. Part 1. The nature and sources of cloud–active aerosols. *Earth–Science Reviews* 89, 13–41.

Awang, M.B., Jaafar, A.B., Abdullah, A.M., Ismail, M.B., Hassan, M.N., Abdullah, R., Johan, S., Noor, H., 2000. Air quality in Malaysia: Impacts, management issues and future challenges. *Respirology* 5, 183–196.

Babu, S.S., Moorthy, K.K., Satheesh, S.K., 2007. Temporal heterogeneity in aerosol characteristics and the resulting radiative impacts at a tropical coastal station–Part 2: Direct short wave radiative forcing. *Annales Geophysicae* 25, 2309–2320.

Chew, B.N., Campbell, J.R., Reid, J.S., Giles, D.M., Welton, E.J., Salinas, S.V., Liew, S.C., 2011. Tropical cirrus cloud contamination in sun photometer data. *Atmospheric Environment* 45, 6724–6731.

DOE (Department of Environment), 2010. Malaysia Environment Quality Report 2010, Chapter 5: Pollution Sources Inventory, Petaling Jaya, Malaysia.

Draxler, R.R., Hess, G.D., 1998. An overview of the hysplit_4 modelling system for trajectories, dispersion and deposition. *Australian Meteorological Magazine* 47, 295-308.

Eck, T.F., Holben, B.N., Sinyuk, A., Pinker, R.T., Goloub, P., Chen, H., Chatenet, B., Li, Z., Singh, R.P., Tripathi, S.N., Reid, J.S., Giles, D.M., Dubovik, O., O'Neill, N.T., Smirnov, A., Wang, P., Xia, X., 2010. Climatological aspects of the optical properties of fine/coarse mode aerosol mixtures. *Journal of Geophysical Research–Atmospheres* 115, art. no. D19205.

Eck, T.F., Holben, B.N., Reid, J.S., Dubovik, O., Smirnov, A., O'Neill, N.T., Slutsker, I., Kinne, S., 1999. Wavelength dependence of the optical depth of biomass burning, urban, and desert dust aerosols. *Journal of Geophysical Research–Atmospheres* 104, 31333–31349.

Gerasopoulos, E., Andreae, M.O., Zerefos, C.S., Andreae, T.W., Balis, D., Formenti, P., Merlet, P., Amiridis, V., Papastefanou, C., 2003. Climatological aspects of aerosol optical properties in Northern Greece. *Atmospheric Chemistry and Physics* 3, 2025–2041.

GSFC (Goddard Space Flight Center), 2014. http://aeronet.gsfc.nasa.gov/cgi-bin/climo_menu_v2_new, accessed in January 2014.

Gupta, P., Khan, M.N., da Silva, A., Patadia, F., 2013. MODIS aerosol optical depth observations over urban areas in Pakistan: Quantity and quality of the data for air quality monitoring. *Atmospheric Pollution Research* 4, 43–52.s

Hansen, J., Sato, M., Ruedy, R., 1997. Radiative forcing and climate response. *Journal of Geophysical Research–Atmospheres* 102, 6831–6864.

Holben, B.N., Tanre, D., Smirnov, A., Eck, T.F., Slutsker, I., Abuhassan, N., Newcomb, W.W., Schafer, J.S., Chatenet, B., Lavenu, F., Kaufman, Y.J., Castle, J.V., Setzer, A., Markham, B., Clark, D., Frouin, R., Halthore, R., Karneli, A., O'Neill, N.T., Pietras, C., Pinker, R.T., Voss, K., Zibordi, G., 2001. An emerging ground–based aerosol climatology: Aerosol optical depth from AERONET. *Journal of Geophysical Research–Atmospheres* 106, 12067–12097.

Holben, B.N., Eck, T.F., Slutsker, I., Tanre, D., Buis, J.P., Setzer, A., Vermote, E., Reagan, J.A., Kaufman, Y.J., Nakajima, T., Lavenu, F., Jankowiak, I., Smirnov, A., 1998. AERONET–A federated instrument network and data archive for aerosol characterization. *Remote Sensing of Environment* 66, 1–16.

Huebert, B.J., Bates, T., Russell, P.B., Shi, G.Y., Kim, Y.J., Kawamura, K., Carmichael, G., Nakajima, T., 2003. An overview of ACE–Asia: Strategies for quantifying the relationships between Asian aerosols and their climatic impacts. *Journal of Geophysical Research–Atmospheres* 108, art. no. 8633.

Ichoku, C., Kaufman, Y.J., Remer, L.A., Levy, R., 2004. Global aerosol remote sensing from MODIS. *Trace Constituents in the Troposphere and Lower Stratosphere* 34, 820–827.

IPCC (Intergovernmental Panel on Climate Change), 2013. Climate change 2013: The Physical Science Basis: Contribution of Working Group I to the Fifth Assessment Report of the Intergovernmental Panel on Climate Change.

IPCC (Intergovernmental Panel on Climate Change), 2007. Climate Change 2007: The Physical Science Basis: Contribution of Working Group I to the Fourth Assessment Report of the Intergovernmental Panel on Climate Change.

Jalal, K.A., Asmat, A., Ahmad, N., 2012. Retrievals of Aerosol Optical Depth and Angstrom Exponent for Identification of Aerosols at Kuching, Sarawak, Hohhot, pp. 5734–5737.

Kaskaoutis, D.G., Kambezidis, H.D., 2008. The role of aerosol models of the SMARTS code in predicting the spectral direct–beam irradiance in an urban area. *Renewable Energy* 33, 1532–1543.

Kaskaoutis, D.G., Kambezidis, H.D., Hatzianastassiou, N., Kosmopoulos, P.G., Badarinath, K.V.S., 2007. Aerosol climatology: On the discrimination of aerosol types over four AERONET sites. *Atmospheric Chemistry and Physics Discusion* 7, 6357–6411.

Kaufman, Y.J., Tanre, D., Boucher, O., 2002. A satellite view of aerosols in the climate system. *Nature* 419, 215–223.

Kumar, S., Devara, P.C.S., 2012. A long–term study of aerosol modulation of atmospheric and surface solar heating over Pune, India. *Tellus Series B–Chemical and Physical Meteorology* 64, art. no. 18420.

Lelieveld, J., Crutzen, P.J., Ramanathan, V., Andreae, M.O., Brenninkmeijer, C.A.M., Campos, T., Cass, G.R., Dickerson, R.R., Fischer, H., de Gouw, J.A., Hansel, A., Jefferson, A., Kley, D., de Laat, A.T.J., Lal, S., Lawrence, M.G., Lobert, J.M., Mayol–Bracero, O.L., Mitra, A.P., Novakov, T., Oltmans, S.J., Prather, K.A., Reiner, T., Rodhe, H., Scheeren, H.A., Sikka, D., Williams, J., 2001. The Indian Ocean experiment: Widespread air pollution from South and Southeast Asia. *Science* 291, 1031–1036.

Levy, R.C., Remer, L.A., Martins, J.V., Kaufman, Y.J., Plana–Fattori, A., Redemann, J., Wenny, B., 2005. Evaluation of the MODIS aerosol retrievals over ocean and land during CLAMS. *Journal of the Atmospheric Sciences* 62, 974–992.

Lin, N.H., Tsay, S.C., Maring, H.B., Yen, M.C., Sheu, G.R., Wang, S.H., Chi, K.H., Chuang, M.T., Ou–Yang, C.F., Fu, J.S., Reid, J.S., Lee, C.T., Wang, L.C., Wang, J.L., Hsu, C.N., Sayer, A.M., Holben, B.N., Chu, Y.C., Nguyen, X.A., Sopajaree, K., Chen, S.J., Cheng, M.T., Tsuang, B.J., Tsai, C.J., Peng, C.M., Schnell, R.C., Conway, T., Chang, C.T., Lin, K.S., Tsai, Y.I., Lee, W.J., Chang, S.C., Liu, J.J., Chiang, W.L., Huang, S.J., Lin, T.H., Liu, G.R., 2013. An overview of regional experiments on biomass burning aerosols and related pollutants in Southeast Asia: From BASE–ASIA and the Dongsha Experiment to 7–SEAS. *Atmospheric Environment* 78, 1–19.

Moorthy, K.K., Beegum, S.N., Srivastava, N., Satheesh, S.K., Chin, M., Blond, N., Babu, S.S., Singh, S., 2013. Performance evaluation of chemistry transport models over India. *Atmospheric Environment* 71, 210–225.

Moorthy, K.K., Babu, S.S., Satheesh, S.K., 2007. Temporal heterogeneity in aerosol characteristics and the resulting radiative impact at a tropical coastal station – Part 1: Microphysical and optical properties. *Annales Geophysicae* 25, 2293–2308.

MOSTI, 2012. http://www.met.gov.my/index.php?option=com_content&task=view&id=75, accessed in December, 2012.

Mukai, S., Sano, I., Satoh, M., Holben, B.N., 2006. Aerosol properties and air pollutants over an urban area. *Atmospheric Research* 82, 643–651.

Okulov, O., Ohvril, H., Kivi, R., 2002. Atmospheric precipitable water in Estonia, 1990–2001. *Boreal Environment Research* 7, 291–300.

Pace, G., di Sarra, A., Meloni, D., Piacentino, S., Chamard, P., 2006. Aerosol optical properties at Lampedusa (Central Mediterranean). 1. Influence of transport and identification of different aerosol types. *Atmospheric Chemistry and Physics* 6, 697–713.

Remer, L.A., Kleidman, R.G., Levy, R.C., Kaufman, Y.J., Tanre, D., Mattoo, S., Martins, J.V., Ichoku, C., Koren, I., Yu, H.B., Holben, B.N., 2008. Global aerosol climatology from the MODIS satellite sensors. *Journal of Geophysical Research–Atmospheres* 113, art. no. D14S07.

Rosenfeld, D., 2007. Aerosol–cloud interactions control of earth radiation and latent heat release budgets, in *Solar Variability and Planetary Climates*, edited by Calisesi, Y., Bonnet, R.M., Gray, L., Langen, J., Lockwood, M., Springer New York, pp. 149–157.

Russell, P.B., Bergstrom, R.W., Shinozuka, Y., Clarke, A.D., DeCarlo, P.F., Jimenez, J.L., Livingston, J.M., Redemann, J., Dubovik, O., Strawa, A., 2010. Absorption angstrom exponent in AERONET and related data as an indicator of aerosol composition. *Atmospheric Chemistry and Physics* 10, 1155–1169.

Salinas, S.V., Chew, B.N., Liew, S.C., 2009. Retrievals of aerosol optical depth and angstrom exponent from ground–based Sun–photometer data of Singapore. *Applied Optics* 48, 1473–1484.

Satheesh, S.K., Srinivasan, J., Moorthy, K.K., 2006. Spatial and temporal heterogeneity in aerosol properties and radiative forcing over Bay of Bengal: Sources and role of aerosol transport. *Journal of Geophysical Research–Atmospheres* 111, art. no. D08202.

Schuster, G.L., Dubovik, O., Holben, B.N., 2006. Angstrom exponent and bimodal aerosol size distributions. *Journal of Geophysical Research–Atmospheres* 111, art. no. D07207.

Seinfeld, J.H., Carmichael, G.R., Arimoto, R., Conant, W.C., Brechtel, F.J., Bates, T.S., Cahill, T.A., Clarke, A.D., Doherty, S.J., Flatau, P.J., Huebert, B.J., Kim, J., Markowicz, K.M., Quinn, P.K., Russell, L.M., Russell, P.B., Shimizu, A., Shinozuka, Y., Song, C.H., Tang, Y.H., Uno, I., Vogelmann, A.M., Weber, R.J., Woo, J.H., Zhang, X.Y., 2004. ACE–ASIA – Regional climatic and atmospheric chemical effects of Asian dust and pollution. *Bulletin of the American Meteorological Society* 85, 367–380.

Smirnov, A., Holben, B.N., Giles, D.M., Slutsker, I., O'Neill, N.T., Eck, T.F., Macke, A., Croot, P., Courcoux, Y., Sakerin, S.M., Smyth, T.J., Zielinski, T., Zibordi, G., Goes, J.I., Harvey, M.J., Quinn, P.K., Nelson, N.B., Radionov, V.F., Duarte, C.M., Losno, R., Sciare, J., Voss, K.J., Kinne, S., Nalli, N.R., Joseph, E., Moorthy, K.K., Covert, D.S., Gulev, S.K., Milinevsky, G., Larouche, P., Belanger, S., Horne, E., Chin, M., Remer, L.A., Kahn, R.A., Reid, J.S., Schulz, M., Heald, C.L., Zhang, J., Lapina, K., Kleidman, R.G., Griesfeller, J., Gaitley, B.J., Tan, Q., Diehl, T.L., 2011. Maritime aerosol network as a component of AERONET – First results and comparison with global aerosol models and satellite retrievals. *Atmospheric Measurement Techniques* 4, 583–597.

Smirnov, A., Holben, B.N., Dubovik, O., Frouin, R., Eck, T.F., Slutsker, I., 2003. Maritime component in aerosol optical models derived from Aerosol Robotic Network data. *Journal of Geophysical Research–Atmospheres* 108, art. no. 4033.

Smirnov, A., Holben, B.N., Dubovik, O., O'Neill, N.T., Eck, T.F., Westphal, D.L., Goroch, A.K., Pietras, C., Slutsker, I., 2002a. Atmospheric aerosol optical properties in the Persian Gulf. *Journal of the Atmospheric Sciences* 59, 620–634.

Smirnov, A., Holben, B.N., Kaufman, Y.J., Dubovik, O., Eck, T.F., Slutsker, I., Pietras, C., Halthore, R.N., 2002b. Optical properties of atmospheric aerosol in maritime environments. *Journal of the Atmospheric Sciences* 59, 501–523.

Smirnov, A., Yershov, O., Villevalde, Y., 1995. Measurement of aerosol optical depth in the Atlantic Ocean and Mediterranean Sea. *Atmospheric Sensing and Modeling II* 2582, 203–214.

Toledano, C., Cachorro, V.E., Berjon, A., de Frutos, A.M., Sorribas, M., de la Morena, B.A., Goloub, P., 2007. Aerosol optical depth and angstrom exponent climatology at El Arenosillo AERONET site (Huelva, Spain). *Quarterly Journal of the Royal Meteorological Society* 133, 795–807.

Tripathi, S.N., Dey, S., Chandel, A., Srivastava, S., Singh, R.P., Holben, B.N., 2005. Comparison of MODIS and AERONET derived aerosol optical depth over the Ganga Basin, India. *Annales Geophysicae* 23, 1093–1101.

Xian, P., Reid, J.S., Atwood, S.A., Johnson, R.S., Hyer, E.J., Westphal, D.L., Sessions, W., 2013. Smoke aerosol transport patterns over the Maritime Continent. *Atmospheric Research* 122, 469–485.